Combined Reconstruction and Motion Correction in SPECT Imaging

Hanno Schumacher, Jan Modersitzki, Bernd Fischer

Abstract— **Due to the long imaging times in SPECT, patient motion is inevitable and constitutes a serious problem for any reconstruction algorithm. The measured inconsistent projection data lead to reconstruction artifacts which can significantly affect the diagnostic accuracy of SPECT if not corrected. To address this problem a new approach for motion correction is introduced. It is purely based on the measured SPECT data and therefore belongs to the data-driven motion correction algorithm class. However, it does overcome some of the shortcomings of conventional methods. This is mainly due to the innovative idea to combine reconstruction and motion correction in one optimization problem. The scheme allows for the correction of abrupt and gradual patient motion. To demonstrate the performance of the proposed scheme extensive 3D tests with numerical phantoms for 3D rigid motion are presented. In addition, a test with real patient data is shown. Each test shows an impressive improvement of the quality of the reconstructed image.**

Index Terms— **motion correction, image reconstruction, SPECT**

I. Introduction

In Single Photon Emission Computed Tomography (SPECT), the imaging time is typically in the range of 5-30 minutes. Here, patient movement, which has frequently been reported in clinical applications [**?**], constitutes a serious problem for any reconstruction scheme. The movements cause misalignment of the projection frames, which degrades the reconstructed image and may introduce artifacts. These motion artifacts may significantly affect the diagnostic accuracy [**?**], [**?**], [**?**]. Different methods have been proposed for the correction of motion in SPECT studies. These methods may be divided into two categories.

The first category includes hardware methods, for example the triple scan [**?**] or dual scan [**?**] protocol. These methods do produce motion corrected projections and thus may be used in conjunction with any reconstruction method. Unfortunately not all types of motion, for example gradual motion, can be corrected. Other methods in this category rely on the placement of some markers on the patient and use camera or tracking systems to detect or estimate patient motion during the SPECT imaging [**?**], [**?**]. Here, in list-mode the position of each detected photon can be corrected directly in conjunction with every reconstruction algorithm. Yet another way is to subdivide the measured data in sets belonging to the same patient position and employing a reconstruction method based on the estimated motion information [**?**], [**?**]. The marker-based approaches clearly decrease the motion artifacts for the price of having to place the markers on each patient and the need for additional equipment.

In this note we advocate the employment of a novel method within the second category, the software methods. These approaches are working solely with the measured raw data. Here one distinguishes between projection- and image-space based approaches. One idea is to reconstruct the image followed by a simulation of SPECT-imaging based on the obtained reconstructed data [**?**], [**?**]. Next, the measured projections and the computed forward-projections are compared in order to estimate and to correct for patient motion in the projection-space. It should be noted, that due to the projection geometry, this method is not able to compensate for rotational movement. Therefore a method, the so called Data-Driven Motion Correction (DDMC) approach [**?**], [**?**], was developed. Here the idea is to estimate the motion and to correct for it within the image-space by applying a registration scheme onto the images obtained by corresponding partial reconstructions. This method can handle full rigid-body motion. Unfortunately it was designed only for SPECT systems with perpendicular camera-heads. Furthermore, the partial reconstructions have to be based on at least 30% of all measured projections as the success of the registration scheme relies on high quality partial reconstruction images. Consequently, the DDMC method can only correct for abrupt patient motion and can not be employed for gradual motion problems.

In this note, we report on a novel motion correction approach, working solely on the raw data, which does overcome the above mentioned shortcomings. The new scheme, which Combines Reconstruction and Motion Correction in one optimization step is called CRMC and was briefly introduced in [**?**]. One may find a similar idea within the super-resolution methodology [**?**], where roughly speaking, the goal is to obtain a ”nice image” out of two or more related ”bad images”. As it turns out, the CRMC approach is able to correct for abrupt and gradual motion. Furthermore, it works successfully with any one-, two-, or triple-head SPECT system. As it is characteristic for inverse problems, the reconstruction process is ill-posed and its formulation and implementation does need special care. To this end we introduce a novel regularization term which overcomes possible problems and works just fine in practice.

The paper is organized as follows. First, a short introduction to the DDMC approach is given. Afterwards we describe on how to combine reconstruction and motion correction in one go. Afterwards the performance of the CRMC approach is demonstrated for a variety of examples including real patient data.

B. Fischer is with the Institute of Mathematics, University of Lübeck, Wallstrasse 40, 23560 Lübeck, Germany. J. Modersitzki is with the Department of Computing and Software, McMaster University, 1280 Main Street West, Hamilton, ON Canada L8S 4K1. H. Schumacher is with the MiE GmbH, Hauptstr. 112, 23845 Seth, Germany.

II. METHODS

Obviously any reconstruction scheme can be improved by correction for patient movement. On the other hand, if one is looking for a correction algorithm based on the reconstructed image, both schemes should learn from each other. Therefore, it is natural to combine reconstruction and motion correction within SPECT imaging.

First, before describing the DDMC method and our new CRMC method, let us introduce some notation. The image to be reconstructed is denoted by $\mathbf{f}$, defined on the set $\Omega_f \subset \mathbf{R}^3$. We assume for simplicity, that it is isotropically discretized with voxel size h_f. Other discretizations are easily dealt with. It is notationally convenient to store the 3D object $\mathbf{f}$ in a (long) vector, which will be denoted by $\mathbf{f} \in \mathbf{R}^{n^3}$ as well. The collection of 2D-projections will be denoted by $\mathbf{g}$. Their pixel size is h_g. Again, we represent $\mathbf{g} \in \mathbf{R}^{q \cdot n^2}$ as a vector, where q denotes the number of projections. Next we introduce the projection matrix $\mathbf{A} = \mathbf{A}_{h_f}$. Its entries describe the probability that an event in voxel i (column) of the image is detected in pixel j (row) of the projections [**?**]. The idea is to simulate the characteristics of the present SPECT-system via the matrix $\mathbf{A} \in \mathbf{R}^{q \cdot n^2 \times n^3}$. It may be used to model the response of the detectors, the structure of the collimator, and scatter or absorption properties [**?**], [**?**]. For the examples to be presented, we are using a simple model without scatter or absorption effects and assume a perfect parallel projection geometry.

A. Data-Driven Motion Correction

The DDMC approach [?], [?] can handle full 3D rigid-body motion (6 degrees of freedom) that occurs between projections. For an approach used in reconstruction of PET images, including motion correction in a single projection see [**?**] and references therein. To start the scheme, it is assumed that the rigid-body motion of the patient is known. The actual determination of the movement is not subject of this paper, see [?], [**?**], for an overview in this direction. Once the motion is known it needs to be corrected. The idea is to subdivide the projection data into subsets where no motion has been detected and to move the object estimate for each of these subsets accordingly. To this end the rigid-body parameters after the ith movement of the patient are stored in the vector $\mathbf{w}_i$. Furthermore, all projections that were measured between the ith and the $i+1$st movement are collected in the projection set $\mathbf{g}_i$. The image, which has been in the course of the algorithm reconstructed up to the ith step, is denoted by $\mathbf{f}^{(i)}$. This image has to be corrected with respect to the next object position $\mathbf{w}_{i+1}$. The result is denoted by $\mathbf{f}^{(i)}(\mathbf{w}_{i+1})$. Next the partial reconstruction $\mathbf{f}^{(i)}(\mathbf{w}_{i+1})$ is updated with the help of measured projections $\mathbf{g}_{i+1}$ via

$$\mathbf{f}^{(i+1)} = \Re[\mathbf{g}_{i+1}, \mathbf{f}^{(i)}(\mathbf{w}_{i+1})], \tag{1}$$

where $\Re$ denotes a reconstruction algorithm. Ideally, the resulting image $\mathbf{f}^{(m)}$ should contain less motion artifacts. An important ingredient in the overall scheme is an interpolation method taking care of the necessary image interpolation in the m steps of the scheme, in particular for the computation of $\mathbf{f}^{(i)}(\mathbf{w}_{i+1})$. Here, we refer to [**?**] and references therein. A widely used reconstruction algorithm is the so-called OSEM algorithm [**?**]. It employs iteratively projection and backprojection in order to calculate a reconstruction based on the actual set of projections. As we are working with discrete data, the projection and backprojection needed in the OSEM scheme may be written in terms of matrices $\mathbf{A}$ and $\mathbf{A}^\top$, respectively. Let $\mathbf{A}_{i+1}$ denote the projection matrix corresponding to the projection set $\mathbf{g}_{i+1}$. The update scheme (**??**) together with the OSEM algorithm may then be conveniently written as

$$\mathbf{f}^{(i+1)} = \mathbf{f}^{(i)}(\mathbf{w}_{i+1}) \cdot \left(\frac{\mathbf{A}_{i+1}^\top \left(\frac{\mathbf{g}_{i+1}}{\mathbf{A}_{i+1}\mathbf{f}^{(i)}(\mathbf{w}_{i+1})} \right)}{\mathbf{A}_{i+1}^\top \mathbf{1}} \right). \tag{2}$$

Here $\mathbf{1} = (1, \ldots, 1)^\top$ denotes a vector corresponding to the size of $\mathbf{A}_{i+1}^\top$. Furthermore, the notation $\mathbf{x} \cdot \mathbf{y}$ and $\frac{\mathbf{x}}{\mathbf{y}}$ indicates a component wise multiplication and division of the vectors $\mathbf{x}, \mathbf{y}$. For convenience, we assume throughout the paper that the denominator has no zero components. Unfortunately the DDMC method was designed only for SPECT systems with perpendicular camera-heads. Furthermore, the partial reconstructions have to be based on at least 30% of all measured projections as the success of the registration scheme relies on high quality partial reconstruction images. Consequently, the DDMC method can only correct for abrupt patient motion and can not be employed for gradual motion problems.

B. Combined Reconstruction and Motion Correction

To descripe our new CRMC method which overcomes the problems of the DDMC approach we start from a reconstruction framework. In the literature one may find analytic as well as iterative method for the reconstruction step, cf. [**?**], [?], [**?**]. Here, we have chosen an iterative approach, as it is much easier to incorporate additional requirements. Ideally, the thought after $\mathbf{f}$ should be a solution of the linear equation $\mathbf{Af} = \mathbf{g}$. This naive approach exhibits several problems. A solution, if at all existing, need not to be unique and is not necessary non-negative $\mathbf{f} \geq 0$, an obvious requirement for measurements. This leads us to the constraint least-squares problem

$$\mathbf{J}_1(\mathbf{f}) = \frac{h_g}{2} \|\mathbf{Af} - \mathbf{g}\|_2^2 \to \min \quad \text{s.t. } \mathbf{f} \geq 0 \tag{3}$$

with the Euclidean vector norm $\|.\|_2$. However, the ill-posedness of the underlying problem, cf. [**?**], [**?**], indicates that the optimization problem (**??**) needs special care, a regularizer has to be introduced, which brings us to

$$\mathbf{J}_2(\mathbf{f}) = \frac{h_g}{2} \|\mathbf{Af} - \mathbf{g}\|_2^2 + \alpha \mathcal{R}_1(\mathbf{f}) \to \min \quad \text{s.t. } \mathbf{f} \geq 0, \tag{4}$$

where $\mathcal{R}_1$ is an appropriate regularizer and α a parameter controlling its influence. In the literature one may find various choices for $\mathcal{R}_1$. For the computed example, we have chosen

$$\mathcal{R}_1(\mathbf{f}) = \frac{h_f}{2} \sum_{j=1}^{3} \|\mathbf{B}_j \mathbf{f}\|_2^2, \tag{5}$$

where $\mathbf{B}_j$ denotes a matrix which encodes a finite difference approximation of the first derivative in the j-th image direction. This choice clearly prefers smooth images and is well suited for handling noisy images, where the regularization parameter α should reflect the present noise-level in the data. Its actual choice is not straightforward and depends on the actual situation. However, the choice $\alpha = 0.01$ works well in all our tests runs. Of course other choices for the regularizer, like for example the total variation functional [**?**], are possible too. The solution of (**??**) may be computed by any sound optimization scheme [**?**] and does provide what we want in the absence of motion artifacts.

The next step it to combine reconstruction and motion correction. To this end, we assume that the measured projections can be divided in K sets, where no patient movement occurred. These subsets are denoted by $\mathbf{g}_i, i = 1, ..., K$. Furthermore, we denote by A_i the portion of A which corresponds to g_i. Now, the partial reconstruction $A_i\mathbf{f}_i \approx \mathbf{g}_i$ would lead to different $\mathbf{f}_i$ reflecting the patient movement. To come up with a single reconstruction $\mathbf{f}$, the idea is to compensate for the motion right away by introducing a transformation $\mathbf{T}(\mathbf{w}_i)$, depending on the parameter set $\mathbf{w}_i$ and solving the combined optimization problem

$$\begin{aligned}\mathbf{J}_3(\mathbf{f},\mathbf{w}) &= \frac{h_g}{2}\sum_{i=1}^{K}\|\mathbf{A}_i\mathbf{T}(\mathbf{w}_i)\mathbf{f}-\mathbf{g}_i\|_2^2 \\ &\quad +\alpha\mathcal{R}_1(\mathbf{f}) \to \min \quad \text{s.t. } \mathbf{f}\geq 0,\end{aligned} \tag{6}$$

where $\mathbf{w}$ denotes the collection of local parameter $\mathbf{w}_i$. Several comments are in order. Depending on the expected patient motion, a corresponding transformation model has to be chosen. Here, we simply use a rigid transformation, based upon six degrees of freedom. However, any other parameterizable model could be used. In general, when applying $\mathbf{T}(\mathbf{w}_i)$ onto $\mathbf{f}$ an interpolation step is required. Here, a tri-linear interpolation is employed. On the first glance, one might get the impression that the precise knowledge of the number K is required. As we will see later on, the correct estimation of the number of motions is not critical for (**??**) and may be overestimated and may be even not related to the projection where a patient movement occurred.

There is still an obstacle connected to the proposed approach which is brought out in the following test run and is depicted in Figure **??**. A synthetic image (top left) is perturbed by motion leading to a motion corrupted reconstruction (top right). Now, the solution of (**??**) is computed with three different starting guesses for the parameter set $\mathbf{w}$. The respective results are displayed in the bottom row of Figure **??**. In each case, the ring is nicely reconstructed. However, its position seems to depend on the starting guess. To overcome this ambiguity, we propose the use of a second novel regularizer

$$\mathcal{R}_2(\mathbf{w}) = \frac{1}{2}\|\frac{1}{K}\sum_{i=1}^{K}\mathbf{w}_i\|_2^2. \tag{7}$$

The idea is to penalizes an offset of the motion parameter and therefore to favor a mean position of the object. The actual value of the regularization parameter β is not critical.

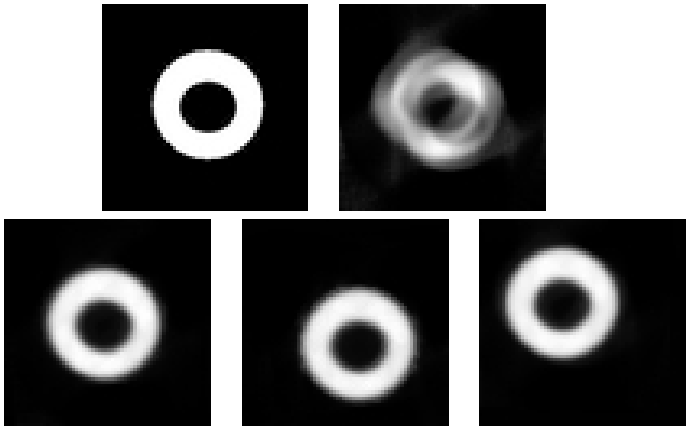

Fig. 1. A SPECT imaging of an numerical phantom (top left) is perturbed with motion (top right). The second row shows three results for the CRMC method starting with different parameter sets $\mathbf{w}$.

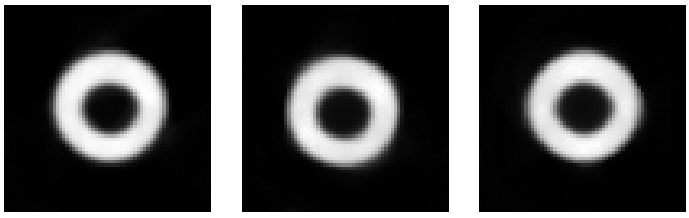

Fig. 2. Results of (**??**) for the three tests presented in Fig. **??**.

We always choose a high value ($\beta = 10^6, 10^7$), in order to ensure its impact.

Altogether, we end up with the optimization problem

$$\begin{aligned}\mathbf{J}_4(\mathbf{f},\mathbf{w}) &= \frac{h_g}{2}\sum_{i=1}^{K}\|\mathbf{A}_i\mathbf{T}(\mathbf{w}_i)\mathbf{f}-\mathbf{g}_i\|_2^2 \\ &\quad +\alpha\mathcal{R}_1(\mathbf{f})+\beta\mathcal{R}_2(\mathbf{w}) \to \min \quad \text{s.t. } \mathbf{f}\geq 0.\end{aligned} \tag{8}$$

To see on whether $\mathcal{R}_2(\mathbf{w})$ does its job, we repeat the previous test case with $\beta = 10^7$. As it is apparent from Figure **??**, the CRMC results no longer depend on the starting guess.

Next, we employ the standard substitution $\mathbf{f} = e^{\mathbf{z}}$ (see, e.g., [**?**], [**?**]) to turn the constraint (**??**) into an unconstrained optimization problem

$$\begin{aligned}J_5(\mathbf{z},\mathbf{w}) =& \frac{h_g}{2}\sum_{i=1}^{K}\|\mathbf{A}_i\mathbf{T}(\mathbf{w}_i)e^{\mathbf{z}}-\mathbf{g}_i\|_2^2 \\ &+\frac{\alpha h_f}{2}\sum_{j=1}^{d}\|\mathbf{B}_j e^{\mathbf{z}}\|_2^2+\frac{\beta}{2}\|\frac{1}{K}\sum_{i=1}^{K}\mathbf{w}_i\|_2^2.\end{aligned} \tag{9}$$

This problem may be attacked by any sound optimization procedure.

Here we advocate the use of a proper Gauss-Newton method [?]. To this end let $\nabla J_5(\mathbf{z},\mathbf{w})$ denote the gradient of J_5. To bypass the need for the computation of the Hessian $\nabla^2 J(\mathbf{z},\mathbf{w})$, it is approximated by the Jacobian $DJ_5(\mathbf{z},\mathbf{w})$ of J_5. As usual, the main part of the iterative scheme is the solution of the following linear system

$$D\mathbf{J}_5(\mathbf{z},\mathbf{w})\begin{pmatrix}\mathbf{z}_u\\ \mathbf{w}_u\end{pmatrix} = -\nabla\mathbf{J}_5(\mathbf{z},\mathbf{w}).$$

To solve this system we follow [**?**] and use a decoupled approach. Here each iteration is divided in two steps. First an update of the image parameter $\mathbf{z}$ is computed with fixed motion parameters, second the motion parameters $\mathbf{w}$ are updated while the image parameters are fixed. Due to the different types (linear image parameter with constraints and non linear motion parameter) of parameters a decoupled approach work better than a coupled one. To solve the linear systems in both parts of the decoupled approach we use the Conjugate Gradient method. Furthermore to speed up the optimization and for a better handling of local minima a multi-level schema is used. Therefore we smooth the projection data and represent them on a coarser resolution. After solving the optimization problem at the coarser level the result is used as a starting guess for the next finer level and so on.

III. Results

To demonstrate the performance of our new CRMC approach, it is compared to the DDMC approach. All implementations are done in MATLAB. Each test was calculated on a standard PC with a 2.13GHz dual core system with 2GB RAM. For a first test, three 2D numerical phantoms were created (see Fig. **??**). Every image is of size 64×64 pixel and perturbed by noise. To simulated noise we used Matlabs random generator to add up to $\pm 20\%$ of the image maximum to each pixel (negative image values are set to zero). For every image we simulate a SPECT imaging with 60 projections and two abrupt rigid movements, one after projection 20 and the other after projection 40. The results for all three tests are presented in Fig. **??**. It shows the original (first column), the reconstruction obtained by 20 steps of the standard Expectation-Maximization (EM) algorithm [**?**] (second column), and the motion correction results of the DDMC (third column) and the CRMC approach (fourth column), respectively.

To start with, both the DDMC and CRMC approach where supplied with the correct motion information, that is, both are working with those three projection sets where no motion occured. The DDMC scheme was stopped after 7 iterations, whereas the CRMC was based on a multi-level scheme with 4 levels and [40, 20, 5, 2] iterations from coarse to fine. In all three cases we have chosen $\alpha = 0.01$ and $\beta = 10^6$. The results in Fig. **??** indicate that the quality of the reconstruction obtained by the CRMC approach is comparable to the one of the DDMC approach, when the correct motion time is known beforehand.

In a clinical setting, no motion information is at hand. Therefore, to run the DDMC scheme, an automatic tool for detecting motion [?], [?] is needed. However, the new CRMC scheme does not need any motion information. To demonstrate this, we run the same tests (cf. Fig. **??**) with $K = q = 60$, assuming that each projection belongs to a new object position. Clearly, this is the only option left to the user when no motion information is available. The results are depicted in Fig. **??**. The quality is comparable to the one obtained with motion information. However, as the method has no information on the original position of the object, a rotation or shift may occur. Again we set $\alpha = 0.01$ and $\beta = 10^6$ and were using 4 levels with [40, 20, 5, 2] iterations.

In the next picture (Fig. **??**) we present a 2D test for gradual motion. It displays the original image, a reconstruction of the motion perturbed imaging using the EM algorithm with 20 iterations, and the result of the CRMC approach. In this case a SPECT imaging with a translation of the object after every projection is simulated. That is, each projection belongs to a different object position. Due to this, the DDMC approach has not enough information for the needed partial reconstruction and can not calculate a motion corrected reconstruction. However, the CRMC approach can also handle this situation and compensates all motion artifacts using 4 levels with [40, 20, 5, 2] iterations, $\alpha = 0.01$, and $\beta = 10^6$.

Next, we turn our attention to 3D tests. To this end, two 3D numerical phantoms, shown in Fig. **??**, are used. Both images are of size $64 \times 64 \times 64$. A SPECT imaging of these images is simulated with 60 projections measured around the object. In a first step no attenuation or scattering is simulated. For both phantoms 21 simulations are performed, one without motion and 20 perturbed by motion. The SPECT imaging is corrupted with one to five rigid motions occurring after different projections. Here the three motion angels are in the range of -10 to 10 degrees and all three translation parameters are between -7 to 7 voxel. The number of motions, the time of motion, and the six motion parameters are determined by the Matlab random generator. For each test, the CRMC method uses a multi-level scheme based on 4 levels with [30, 20, 6, 2] iterations, $\alpha = 0.01$, and $\beta = 10^6$.

First the motion free case of the two numerical phantoms is reconstructed with the CRMC approach without motion correction. Later, these reconstructions will be used to evaluate the results of the CRMC approach. Next, the 40 motion corrupted SPECT simulations are also reconstructed without motion correction. To measure the error between the motion free and the motion corrupted case we first use a rigid registration to fit the motion corrupted reconstruction to the motion free one, see, e.g., [**?**]. After the rigid registration the distance measure

$$D(\mathbf{f}^{ref}, \mathbf{f}^{tmp}) = \frac{\sum_i^N |f_i^{ref} - f_i^{tmp}|}{2 \cdot \sum_i^N f_i^{ref}} \cdot 100 \qquad (10)$$

is used to measure the difference, where N denotes the total number of voxel. This error measure can be interpreted as the misplaced radioactivity in percent.

Next the 40 motion corrupted SPECT simulations are reconstructed under the assumption that the correct motion time is known. This takes up to 5 min for each test. Again, these results are compared to the motion free case. Therefore these images are fitted to the motion free case by a rigid registration before using (**??**). Finally, the CRMC method is applied to all 40 cases without any prior information, that is $K = 60$ is used. Due to the higher number of motion parameters this takes about 20 min for each test. Again these results are compared to the motion free case. All results are collected in table **??**. An overview of the tested motion scenarios can be found in table **??**. As it is apparent from table **??** and **??**, the CRMC approach shows impressing results. In all 40 cases the influence of the motion artifacts could be reduced significantly, even when the motion time is not known. To

Original Reconstruction DDMC CRMC

Fig. 3. SPECT imaging of three numerical phantoms (Original) perturbed by abrupt rigid motion and reconstructed with the EM algorithm (Reconstruction), the DDMC and the CRMC approach.

Fig. 4. Motion correction with the CRMC approach of the examples of Fig. **??** with $K = 60$ subsets.

Original Reconstruction CRMC

Fig. 5. SPECT imaging of an numerical phantom (left) which is perturbed by gradual motion. The middle image shows an EM reconstruction and the right image the one obtained by the CRMC scheme.

Fig. 6. The 3D numerical phantoms from different views.

Phantom 1		
Reconstruction	CRMC, known subsets	CRMC, unknown subsets
41.74 ± 10.30	6.76 ± 1.90	8.19 ± 1.63
Phantom 2		
Reconstruction	CRMC, known subsets	CRMC, unknown subsets
21.21 ± 7.12	2.97 ± 1.57	3.51 ± 1.12

TABLE I

MEAN ERROR AND STANDARD DEVIATION IN PERCENT BETWEEN MOTION FREE RECONSTRUCTION AND MOTION CORRUPTED RECONSTRUCTION AND THE CRMC RESULTS WITH AND WITHOUT MOTION INFORMATION. THE ERROR IS MEASURED WITH (**??**). THE FIRST THREE ROWS REPRESENT THE RESULTS OF THE FIRST PHANTOM, THE LAST THREE ONES FOR THE SECOND PHANTOM.

Phantom 1							
#	projection	t_x	t_y	t_z	r_x	r_y	r_z
6	5	0.0	3.1	−6.2	−3.5	−6.4	2.5
	13	0.5	−0.4	−7.0	−7.6	0.5	7.6
	40	−1.2	5.9	3.5	3.9	2.2	−4.9
	52	−4.8	5.3	−0.9	−7.9	−8.5	2.6
8	14	−6.8	−4.5	3.5	−7.1	6.4	−2.2
	29	−3.1	−0.8	−5.5	3.4	−5.0	7.9
	32	0.2	−6.4	−6.2	7.5	7.9	−9.7
10	45	3.9	5.9	2.9	−3.2	−5.5	1.4
	33	5.9	0.9	5.4	−9.6	−6.0	−5.8
	45	3.9	5.9	2.9	−3.2	−5.5	1.4
Phantom 2							
#	projection	t_x	t_y	t_z	r_x	r_y	r_z
13	7	−3.5	5.2	0.2	8.9	8.3	2.0
	27	−6.0	0.7	−2.9	4.7	−1.6	9.2
	39	−6.2	−2.0	0.0	7.2	−3.3	3.6
	49	−5.4	5.6	3.6	−1.3	1.2	2.3
18	7	3.6	6.3	0.8	−2.7	−3.9	7.0
	28	6.7	−3.9	2.9	−9.7	1.9	6.3
7	7	2.8	3.2	−0.3	−2.9	−6.9	3.5
	28	3.0	5.5	−3.2	1.0	−7.6	−1.0
	42	4.2	5.7	−3.8	−4.9	7.3	−5.4

TABLE II

SOME MOTION SENARIOS FOR BOTH PHANTOMS. IT IS PRESENTED AFTER WHICH PROJECTIONS A MOTION OCCURS AND THE USED MOTION PARAMETERS IN PIXEL (TRANSLATION t_x, t_y, t_z) AND DEGREES FOR EACH AXIS (ROTATION r_x, r_y, r_z)

underscore the results from Table **??** the worst examples are displayed in Fig. **??**, namely test 5 for the first and test 18 for the second virtual phantom.

Finally we present an example using real-patient data. It shows the feet of a patient, which had a tremor resulting in several feet movements during the acquisition. 64 projections were acquired with a one-head SPECT using a full 360 degree rotation around the patient. The CRMC method was started with the assumption that each projection belongs to a new position. A reconstruction of these data with and without motion correction, each $128 \times 128 \times 128$ voxel, is shown in Fig. **??**. The 3D images are generated using a volume rendering with a threshold of 2 for the background and 25 for the tumor. The 2D images are displayed using an offset in the colour map to seperate the object contour an the background. It can be seen that the contours of the feet are sharper and the shape of the tumor has changed after motion correction. The improved quality of the result is confirmed by the MiE company which provides the data available.

IV. DISCUSSION

We presented a new approach for motion correction in SPECT imaging, which can correct abrupt and gradual rigid object motion. The approach combines reconstruction and motion correction and uses solely the measured SPECT raw data. The performance of the new approach was demonstrated for numerical phantoms in 2D followed by extensive 3D test runs. In all cases the CRMC approach came up with meaningful motion corrected reconstructions. Furthermore it is demonstrated that the novel approach does not need any prior information on the motion time. Due to this extraordinary feature, the CRMC can be used as a fully automatic motion correction method. On the other hand, however, the computation time depends on the number of assumed projection sets, that is, the scheme would benefit from any user knowledge. Therefore it is intended to combine our scheme with automatic motion detection methods to gain a fast fully automatic data-driven motion correction scheme. Future work will also include the

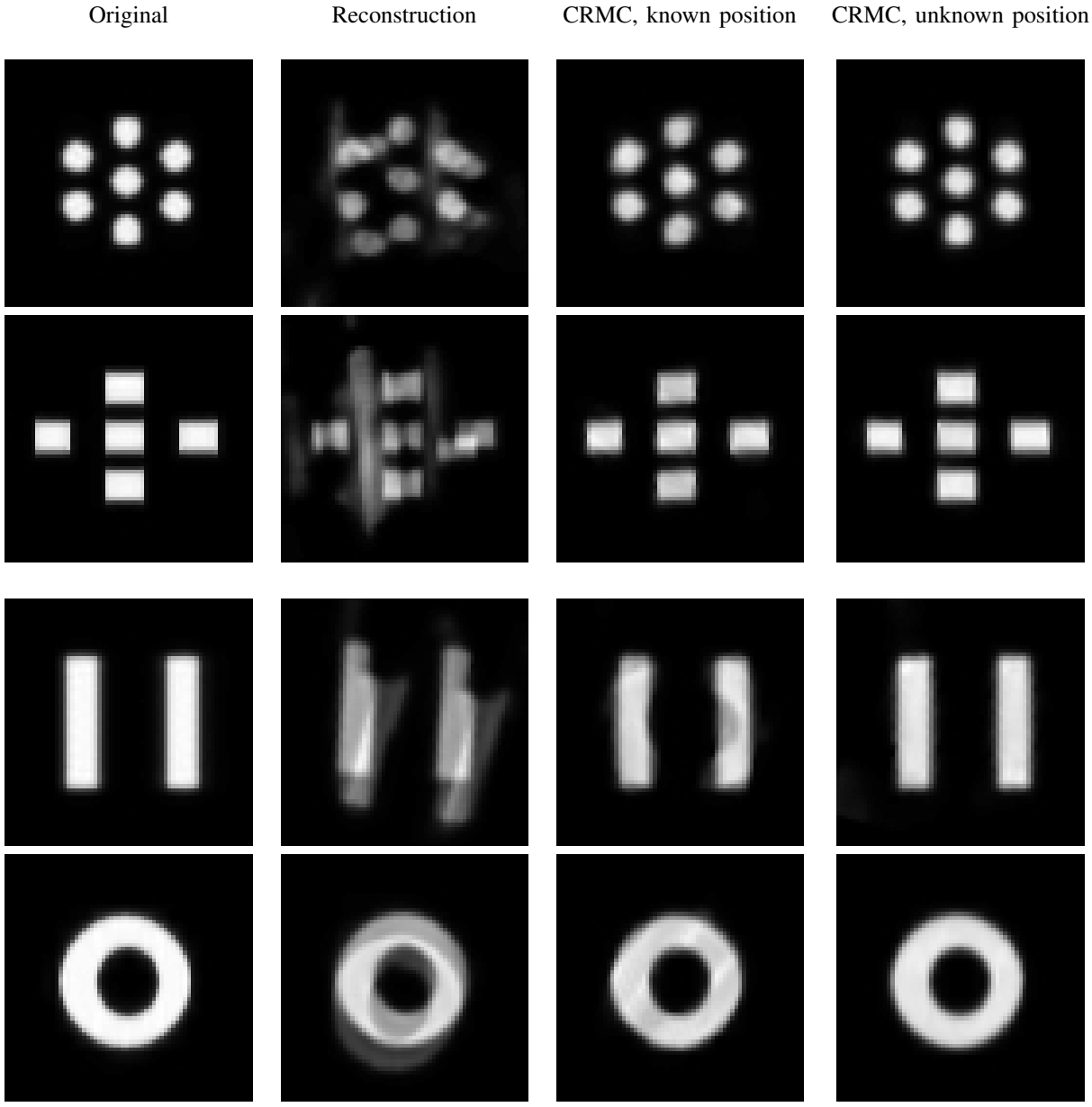

Fig. 7. A SPECT imaging of both 3D numerical phantoms (left) is perturbed with abrupt rigid motion and reconstructed without motion correction (middle left). The results of the CRMC approach with (middle right) or without (right) knowing the motion time indicate its capability of compensating for motion artefacts.

improvement of the optimization scheme by using multi-scale techniques within the multi-level approach. Additionally other regularizers for handling the noisy SPECT data or the motion parameters should be tested.

ACKNOWLEDGMENT

The financial support of both the Innovationsstiftung Schleswig Holstein and the MiE company is gratefully acknowledged. Furthermore, we would like to thank the MiE company for real SPECT data and evaluating our results. Finally, we are grateful to the referees for their useful comments.

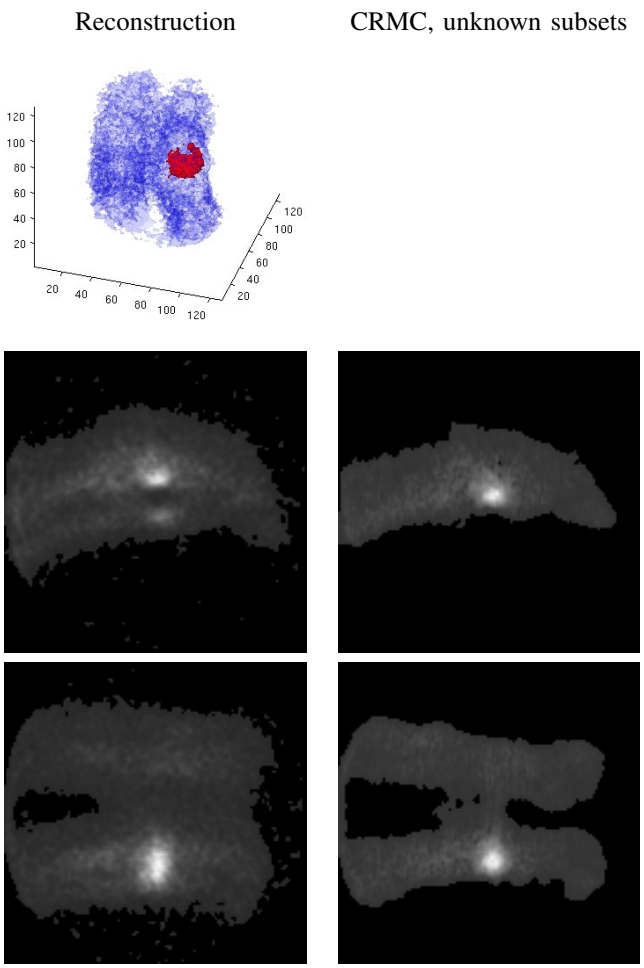

Fig. 8. Volume rendering of reconstructed SPECT feet data without (top) and with motion correction (bottom). Additionally two 2D slices (xz- and yz-plain) are shown.